Nov. 2013, Volume 7, No. 11 (Serial No. 72), pp. 1423-1432
Journal of Civil Engineering and Architecture, ISSN 1934-7359, USA

Use of Geophysical Techniques for the Localization of the Restricting Zones of Permeability in the Bottom of Basin: Forecasting the Zones of Clogging

Ibrahim Alimi Ichola[1], Salima Bouchemella[2] and Claudio Fernando Mahler[3]

1. Laboratoy of Civil Engineering and Environment, Villeurbanne 69621, France

2. Department of Civil Engineering, Guelma and Infrares Laboratory, Guelma 24000, Algeria

3. Waste Technology Study Group, Federal University of Rio de Janeiro, Rio de Janeiro 22470-050, Brasil

Abstract: Measurements of dielectric parameters followed by permeability tests are performed on soil samples of infiltration basin. The dielectric parameters are obtained by TDR (time domain reflectrometry) measurements from which it is found that the measurement of the permittivity, the electrical conductivity and the relaxation time of compacted soil allows the mapping of the values of the coefficient of permeability at the surface of an infiltration basin. With the distribution of the coefficient of permeability, the areas of water stagnation can be detected before the basin filling. The study proves that the TDR measurements for the detection of these zones can be used for the management of infiltration basins for sustainable working and their remediation can be undertaken before the rainy seasons.

Key words: Permeability, infiltration pond, soil conductivity, TDR method.

1. Introduction

The geophysical techniques were mainly developed for detection of in-depth anomalies of sites. For the past few decades, these techniques have been used to detect or localize the pollution in the soil and the ground water within old sites of industrial activities. Analysis of the parameters used in the most of the geophysical techniques can be described by the Debye relaxation function representing the expression of the complex permittivity. The success of the geophysics methods for the site survey rests mainly on the fact that the soil is a dispersive medium and that its' dependence on frequency has the advantage that the contribution of the bulk material and the grain boundaries in the measurements can be distinctly separated. Thus different models of relaxation dielectric are proposed for analysing the dielectric medium response. These models introduce the relaxation frequency or time, the real static permittivity and the real permittivity at infinity frequency.

TDR (time domain reflectrometry) measurements are developed to detect faults in the transmission line. Topp et al. [1] and several other authors that pursued similar research proposed methods of determination of dielectric constant and electrical conductivity of soil surrounding a transmission line. As already shown [2], there exist realistic possibilities of determining the hydraulic conductivity from the results of vertical electric soundings. Consequently, many calibration tests are carried out on samples from the infiltration basin by dielectric and electrical conductivity measurements applying the TDR method. Standard permeability tests are then performed on the samples after TDR measurements. Subsequently, a mapping of the infiltration basin bottom is carried out according to a predetermined grid, by adopting TDR measurements.

Corresponding author: Ibrahim Alimi Ichola, Ph.D., associate professor, research fields: geotechnic-geophysic in unsaturated soils, water and pollutant migration in vadose zone. E-mail: ibrahim.alimi-ichola@insa-lyon.fr.

2. Soil Dielectric Properties

2.1 Complex Permittivity of Dielectric Material

Every material has electrical characteristics which depend on the dielectric properties. Measurement techniques of these properties offer to research engineers the means to ameliorate their quality or control their fabrication. Basically, the dielectric properties of such materials are represented by the electrical resistivity, the permittivity and by the magnetic permeability. These properties change with temperature, pressure, composition and the molecular structure of the material. Fundamental definitions of the basic properties are as follows:

- Electrical conductivity concerns the ionic flow in the material, high resistivity characterizes insulator material, whereas weak resistivity characterizes electrical conductor material;
- Material dielectric constant: A material is called dielectric when it is able to store energy and to restore it, the dielectric constant is the ratio between the capacitor capacity in void and in dielectric material;
- Material permittivity describes the interaction between a material and an applied electric field, the dielectric constant measures the ratio between the permittivity of the material and the permittivity of the void;
- Loss phase: occurs when the permittivity of the material is a complex number represented by a vector. The relative energy loss is the ratio between the restored energy and the stored energy. In this case, the real part of the material permittivity describes the energy storage capacity and the imaginary part describes the energy loss.

All geophysical methods use the electrical flow or the EM (electromagnetic) propagation to reveal the dielectric properties of soil. The change in the value of the measured parameters allows for contrast identification.

The complex permittivity of the material where electrical conductivity is represented as σ is expressed as:

$$\varepsilon^{*} = \varepsilon' - j\left(\varepsilon_{d}'' + \frac{\sigma}{\omega\varepsilon_{0}}\right) \tag{1}$$

where, ε' is the real part of the complex permittivity and ε_d'' is the dielectric loss through energy dissipation.

$\omega = 2\pi f$ is the angular frequency and ε_0 the void permittivity.

The Debye relaxation function allows writing the complex permittivity of insulator material as:

$$\varepsilon^{*} = \varepsilon_{f \to \infty} + \frac{\Delta\varepsilon}{1 + jf / f_{r}} \tag{2}$$

$\Delta\varepsilon = \left(\varepsilon_{f\to 0} - \varepsilon_{f\to\infty}\right)$ defines the difference between the polarization under static field $\varepsilon_{f\to0}$, and the polarization distortion $\varepsilon_{f\to\infty}$. f is the frequency of the electrical field and f_r the relaxation frequency. From the relaxation function, the real and imaginary parts of the complex permittivity are given by:

$$\varepsilon' = \varepsilon_{f \to \infty} + \frac{\Delta\varepsilon}{1 + \left(f / f_{r}\right)^{2}} \tag{3}$$

$$\varepsilon'' = \frac{\Delta\varepsilon\left(f / f_{r}\right)}{1 + \left(f / f_{r}\right)^{2}} + \frac{\sigma}{2\pi f\varepsilon_{0}} \tag{4}$$

The derivative of the Eq. (4) as a frequency function, proves that the loss ε'' is maximum at the frequency of relaxation f_r or at a relaxation time $\tau_r = 1/f_r$.

The Debye relaxation function proves that the dielectric properties of materials can be described in frequency domain or in time domain. Each description domain presents its advantage and its inconveniency.

2.2 Dielectric Property Analysis in Frequency Domain

The variation of the electrical characteristics is provided by the study of the microscopic properties of the materials. For most types of soil, the real part of the permittivity ε' is constant for a frequency less than 2 GHz. The variation of the electrical conductivity σ depends on the frequency bandwidths. As a

consequence, there is a need to choose the study frequency in these respective frequency bandwidths to detect anomalies in the soil. The spectra of the material must be determined to highlight the measurement frequencies. Devices for such measurement are expensive and difficult to implement in situ.

2.3 Dielectric Property Analysis in TDR

A system TDR can be broken up into a signal $u(t)$ injected into a cable represented by a function $h_2(t)$, a probe and the medium tested, $h(t)$ and a cable of exit for recording $h_2(t)$. So Gemert [3] suggests, the reflected signal $r(t)$ is the convolution product given by:

$$r(t) = \int_{-\infty}^{t} u(t-\tau)h(t)d\tau \quad (5)$$

The use of the Fourier transform results in EM propagation within the frequency domain expressed as follows:

$$R(f) = H(f)U(f) \quad (6)$$

It is derived that most part of the signal is valid for a frequency in the range of minimum frequency f_{min} and maximum frequency f_{max}. f_{max} is related to the rise time of the signal which depends on the generator capacity and on the pulse velocity in the cable. $H(f)$ is the transfer function of the probe in the soil. According to Clarkson et al. [4], $H(f)$ depends on soil dielectric properties and the cable impedance and can be obtained from the Eq. (6). Using the model as the Debye model, the soil permittivity can be computed for each frequency. Based on the spectrum of the permittivity thus obtained and the use of the Cole-Cole representation $\varepsilon' = f(\varepsilon'')$, the four parameters of the Debye model can then be determined. The curve $\varepsilon' = f(\varepsilon'')$ and these parameters characterize the dielectric properties of the soil and reveal any change in their structure and their texture.

Fig. 1 presents three types of responses of TDR system corresponding to an open circuit where the coefficient of reflection is 1, a short circuit where the coefficient is -1 and the reflection of the signal in

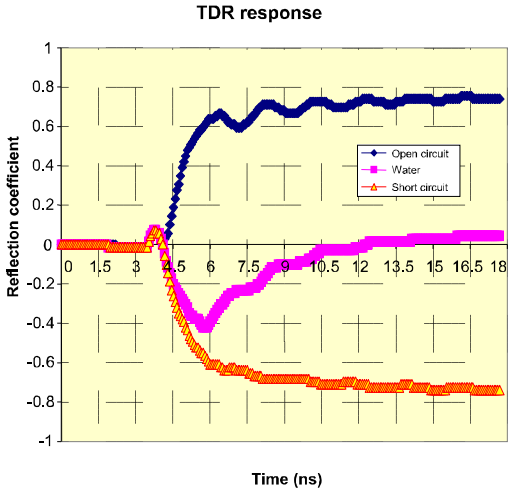

Fig. 1 TDR response $r(t)$ for three media.

water. The transform of Fourier applied to the such curves gives the spectrum $H(f)$ of the response of the medium tested. The real part of the dielectric permittivity, the relaxation frequency and the electric conductivity of the medium tested are the parameters selected to differentiate the mediums. While referring to the works of Topp and Davis [5], Nadler et al. [6], Dasberg and Dalton [7] and Heimovaara et al. [8], the three parameters are directly determined from signal TDR without using the spectrum.

2.4 Dielectric Property Measurement in TDR

Instead of seeking the transfer function of a probe and a medium $H(f)$, the TDR technique consists of launching a high EM wave in the probe and determining the transit time of this wave. A reflection is created at the top of the probe and a second reflection is created at the end of the probe. Since the probe length is fixed, the propagation velocity can be computed as twice the length divided by time required for a pulse to travel along the probe and back. The apparent dielectric constant of the medium is simply a ratio between this measured velocity and the speed of light in free space. The apparent dielectric constant which is the relative real part of the permittivity can be computed by:

$$\varepsilon_r = \left(\frac{c}{v}\right)^2 = \left(\frac{ct}{2L}\right)^2 \quad (7)$$

where, t is the transit time, L the length of the probe and c light speed in free space.

The load Z_L of the transmission line embedded in the investigated soil can be calculated from the voltage reflection coefficient ρ defined by:

$$\rho = \frac{Z_L - Z_0}{Z_L + Z_0} \quad (8)$$

where, Z_0 is the characteristic impedance of the cable, The ρ values can be read directly from the signal curve for longer propagation time. On the other hand, the load Z_L can be calculated and converted to σ_a by using probe's geometric constant. The geometric constant K_c, is experimentally obtained by immersing the probe in a solution of known salinity σ_a, measuring the resistance of Z_L by TDR, and using an equation identical to that proposed by Rhoades and Schilfgaarde [9]:

$$K_c = \sigma_{ref}(25\,^\circ)Z_L / f \quad (9)$$

where, f is temperature correction, σ_{ref} (25 °C) is the permeate electrical conductivity.

The signal TDR response results in a step pulse which undergoes a transformation with the rise in time corresponding to the maximum frequency that the spectrum of the signal contains. The rising part of the signal corresponds to a gain of energy similar to the loading of a capacitor. At the half of the relaxation time the 63% of the maximum loading of the capacitor is attained. It is observed that the point of measurement of the time or the frequency of relaxation is at the 2/3 of the maximum gap between the incident voltage and reflected voltage.

To map out the infiltration basin surface, standard permeability tests based on TDR measurements are carried out in laboratory to determine how electrical parameters correlated to compacted soil permeability.

3. Devices and Soil Tested in Laboratory

3.1 Infiltration Pond

A pond of 4,800 m^2 of bottom surface with storage volume of 44,800 m^3 is built at 10 km from Lyon (France) to infiltrate the storm water runoff. It receives water from a catchment of 119 ha and the soil layer is glacio-fluvial alluvia. The water table depth in this area is 13 m from the basin bottom. Fig. 2 presents a photo of the pond.

Clogging zones observed on the infiltration basin bottom reveal the surface variation of the hydraulic conductivity of the subsoil. Infiltration surfaces without clogs and with clogs are shown in the Figs. 3a and 3b. Sampling was carried out in such zones for laboratory tests.

3.2 Soil Identification

Laboratory tests to determine geotechnical engineering parameters were carried out on the different types of soil extruded from the pond. The results of the tests facilitate for the identification of the samples of soils which characterize the geological formation of the site including the state of pollution of the sampling zones.

3.2.1 Grain Size Distribution

Unscreened samples taken from the basin are defined within the 0/80 mm range in size. The color and the texture of the samples prove that they can be categorized as clean alluvia, polluted alluvia and polluted sands. Three tests were carried out on each type of sample. Grain size distribution curves are shown in Fig. 4. The grain size distribution curves presented in Fig. 4, show that the clean and polluted unscreened soils (0/80 mm) are clean poorly graded

Fig. 2 One of the perspective of the infiltration pond.

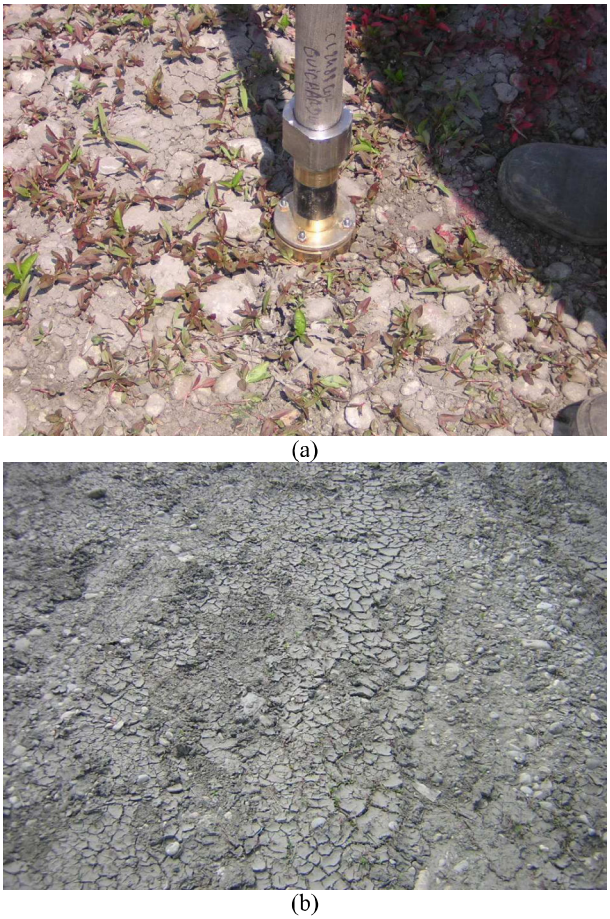

(a)

(b)

Fig. 3 Infiltration surfaces without clogs and with clogs: (a) infiltration surface without clogs; (b) clogging zone of the infiltration surface.

gravel. The sand is clean sand poorly graded. It can be noted that the difference between the two gravels is exhibited in the range of grain size 0.1 mm-10 mm (Fig. 4). The three types of soils, however, contain virtually equal quantities of fines with the sandy soil having a slightly higher content. It is observed, from the grains size distributions that the two alluvia have a high coefficient of permeability. However, the value of this coefficient depends on the unit weight of the earth in place.

3.2.2 Compaction Tests

In order to determine the maximum bulk dry density that can reach the layers of alluvia and of sand, compaction tests were carried out on the three types of samples. The values of the maximum dry density (γ_{dOPN}) with the corresponding optimal water contents (w_{OPN}) are given in Table 1.

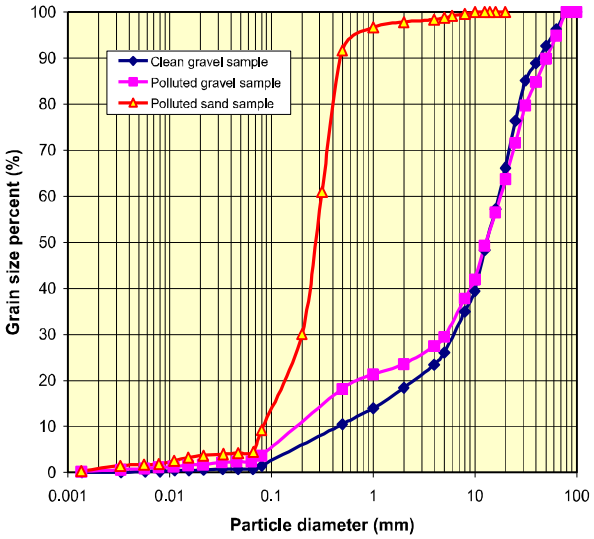

Fig. 4 Grain size distributions for the three types of soil.

Table 1 Compaction test results.

Tested sample	w_n (%)	$(\gamma_d/\gamma_w)_n$	w_{OPN} (%)	$(\gamma_d/\gamma_w)_{OPN}$
Clean alluvia	2.6	1.990	5.8	2.060
Polluted alluvia	5.0	2.000	7.5	2.056
Polluted sand	7.8	1.666	10.0	1.700

w_n: the natural water content of the soil; $(\gamma_d/\gamma_w)_n$: the bulk dry density at the natural water content; w_{OPN}: the water content at the maximal dry density; $(\gamma_d/\gamma_w)_{OPN}$: the maximal bulk dry density.

It can be noted that the two samples of the alluvia have approximately the same maximum bulk dry density but varying optimum water contents, where it is higher for the polluted alluvia. Proctor curves of the two alluvia have the same shape that of the polluted soil is being shifted towards the higher compaction water contents.

Polluted fine sand is characterized by a curve "stretched" with the rather low value of maximum dry density (1.700) and high corresponding water content (10%).

The permeability of the compacted soils and the dielectric properties are correlated based on TDR measurements and permeability tests carried out in the laboratory on compacted samples.

3.3 Permeability and TDR Measurements

In order to characterize the zones of permeability restriction on the surface of the basin, the samples of

soil are compacted in moulds at different water contents and at standard proctor energy. After a TDR measurement, the permeability test on the sample is carried out.

3.3.1 Laboratory TDR Measurements

A TDR probe with five stems able to be inserted in ground is used for the tests. Calibration in water and in a saline solution was undertaken. A cable tester of model Tektronix 1502C connected to a computer allows the production of a signal which is recovered by the units' automatic acquisition program. The results of the calibration are presented in Fig. 1.

Fig. 5 presents an example of the TDR signals which allow for the determination of parameters that characterize dielectric properties of soils. In this figure, the stationery points of inflection indicated are characteristic for the determination of the different parameters. Point A indicates the exit of the signal from the cable while point B corresponds to the contact point between the probe and the soil. The distance BD represents the duration of the rise of the EM signal that traverses the soil. On the other hand, point C, which is the inflection point of the rising part of the curve, corresponds to the exit of the signal from the probe. The time elapsed between A and C signifies the transit time of the wave in the probe. Point D represents the relieve signal towards the end, indicating the time necessary for the loads to locate before the application of the electric fields.

With the Tektronix 1502C cable tester, the minimum and the maximum frequencies are respectively given by:

$$f_{\min} = \frac{cV_p}{2\Delta xN} \quad (10)$$

and

$$f_{\max} = \frac{250\ cV_p}{2\Delta x} = \frac{250\ cV_p}{2\,dd\ .ds} \quad (11)$$

where, Vp is the rate of propagation of the EM wave in the cable, (Vp = 0.659), dd is the scale chosen to display the TDR curve, d_s is the number of points contained in the length of the scale (d_s = 25).

When the scale in distance of 0.25 m is used, the minimum and the maximum frequencies are:

$$f_{min} = 15.8 \text{ MHz and } f_{max} = 3.95 \text{ GHz} \quad (12)$$

The TDR signal for the saline solution resulted the estimated geometric constant of the probe: K_c = 736.

The minimum and maximum values obtained for the three types of samples compacted in the ring of the test of permeability are given in Table 2.

In all cases, the following conclusions can be derived from the results of the TDR measurement:

(1) The dielectric constant increases with the increase in water content, increases when the dry density decreases and is higher in sand than in the alluvial soils;

(2) The relaxation time increases with the increase in water content, decreases when the dry density increases and is higher in sand than in alluvial soil, with higher values recorded in polluted alluvial than in clean alluvial soils;

(3) Electrical conductivity increases with the increase in water content as well as with the dry density and is higher in sand and in polluted alluvial than in clean alluvial soils.

The correlation of these results with the coefficient of permeability is to enable us to differentiate the

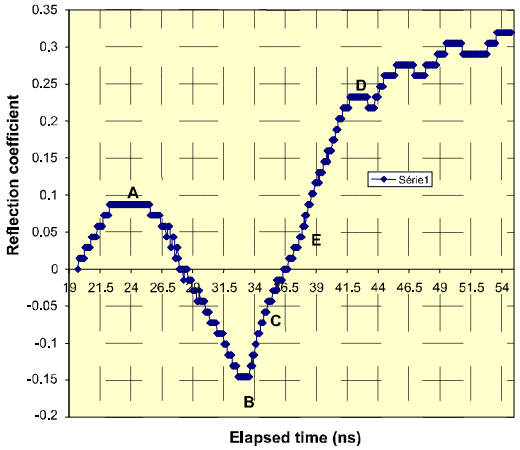

Fig. 5 Model of waveform to determine dielectric parameters.

Table 2 TDR measurements after compaction test.

Values	Θ (%)	τ_r (ns)	ε	σ (mS/m)	γ_d/γ_w
Minimum	6	1.42	3.3	425	1.63
Maximum	26.5	2.12	14.3	958	2.06

measurement points of the surface of the basin.

3.3.2 Laboratory Permeability Tests

The permeability of each material was given according to the water content and dry density of the material and a correlation between the permeability of soil layers and TDR measurements was established. Single values of water content on either of the dry side and wet side were chosen on the Proctor curve of each material in order to limit the number of the permeability tests. The values of the coefficients of permeability are then related to the values of the dielectric parameters. To appreciate this correlation, the various parameters are summarized in Table 3.

The results presented in Table 3 also show the difficulty of saturating the three types of soils by infiltration. But the values of the coefficient of permeability thus determined are indicative of the rate of the infiltration of the water in the basin. When the dielectric parameters are compared to the coefficients of permeability it can be noted that the coefficient of permeability increases when:

(1) the initial water content decreases;

(2) the dielectric constant decreases;

(3) the electrical conductivity decreases;

(4) the relaxation time increases;

(5) the dry density increases.

Among the dielectric parameters which can be used to locate the zones of weak permeability, the permittivity and electrical conductivity have the widest field of variation with change in the permeability coefficient. These two dielectric parameters can help detect in situ, the nature of the soil from the range of the dry density obtained and by giving the order of magnitude of the coefficient of permeability of the ground in place.

Table 3 Comparison of the different parameters.

Soils	Clean alluvia		Polluted alluvia		Polluted sand	
wi (%)	5.1	7.4	5.0	9.0	7.8	14.5
wf (%)	10.2	7.8	9.7	10.0	19.8	15.2
Sr (%)	94.1	66.6	79.8	81.5	89.2	65.9
γ_d/γ_w	2.053	2.018	2.00	1.99	1.67	1.63
ε	4.83	5.89	5.52	8.29	6.25	14.35
σ (mS/m)	454	425	515	668	804	958
τ_r (ns)	1.57	1.62	1.57	1.87	1.67	2.12
10^5k (m/s)	5.1	2.4	4.7	1.5	6.1	3.1

4. In Situ Dielectric Parameter Measurements

For reference and comparative analysis of the state of compactness of the soil layer in the infiltration basin, the measurements of dry density and water content were also carried out using the gamma ray probe method. To fix the measurement points, a grid of the surface of the basin was drawn in plan form of localization. Fig. 6 presents the map of the basin of infiltration with the grid of measurements. The grid on this chart is characterized by its shape in "L", one side considered the small and the other the large wing of the chart for purposes of locating and describing the results.

4.1 Bulk Dry Density Mapping by Gamma Ray Measurement

Measurements of the dry density and of the water content also allow an estimate of the permittivity of the soil layer. It was noted that the values obtained for the density varied from 1.4 to 2.2 and from 3% to 40% for the water content. But these values do not make it possible to distinguish the clean alluvia from the polluted alluvia.

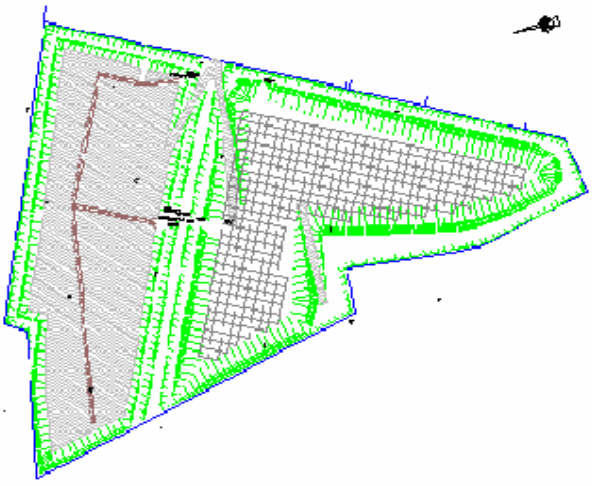

Fig. 6 Presentation of the infiltration basin map.

It was observed that in the small wing of the grid corresponding to the north-west of the basin, the dry density was between 1.4 and 1.7 while the water content was very high from 20% to 40%. This means that the soil layer of this zone is mainly made up of sand. In the central zone, the dry density value is 1.8 and the water content varies from 3% to 7%. These values characterize the nature of the alluvial soils.

The measurements carried out within the large wing of the basin, in the north-south direction enable us to appreciate the presence of various zones. Mainly, in this regard, the existence of high to very high values of density with the relatively low corresponding water contents (between 5%-6%) and exceeding 8% in some case, can be observed intermittently. The presence of alluvia is noted in the greater part.

It is then necessary to compare the various observations with the indicative results given by the dielectric parameters.

4.2 Basin Surface Mapping by Dielectric Constant Measurement

The varying colors of the grid points plotted in Fig. 7 indicate the values of the permittivity within the tested zone. The yellow color corresponds to the lowest value (2 to 4), the red color (from 4 to 6), the green color (high values of 6 to 8) and the blue color (very high value greater than 8). The distribution of the points of color in the north-west part of the basin, covered by polluted fine sand, is characterized by rather high permittivity (color red or green). It can be concluded, according to the already established correlations, that this is a zone of weak dry density with high water content. The whole of the north-south part of the basin (large wing of the basin), covered mainly by alluvia, exhibits various values of permittivity. The colors of the points of measurements confirm the fact that the values of the permittivity are low to medium. Comparison of these results with measurements from the gamma ray probe indicates a good correspondence between the values of the permittivity and the dry density measured by the gamma ray probe. One can thus use these measurements of permittivity to appreciate the compactness of the soil layer.

4.3 Basin Surface Mapping by Electric Conductivity Measurement

The distribution of the values of electrical conductivity is characterized by three level of color. The green color corresponds to the low value (of 0 to 700 mS/m), the dark blue, to a median value (of 700 to 1,200 mS/m) and the light blue color to values ranging between 1,200 and 1,300 mS/m (Fig. 8). In the north-west and extreme east zones of the basin the electrical conductivity lies between 1,200 and 1,300

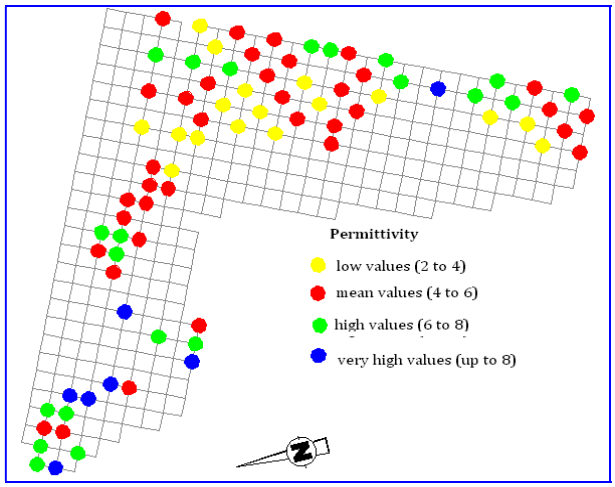

Fig. 7 Distribution of the dielectric constant on the surface of the infiltration basin.

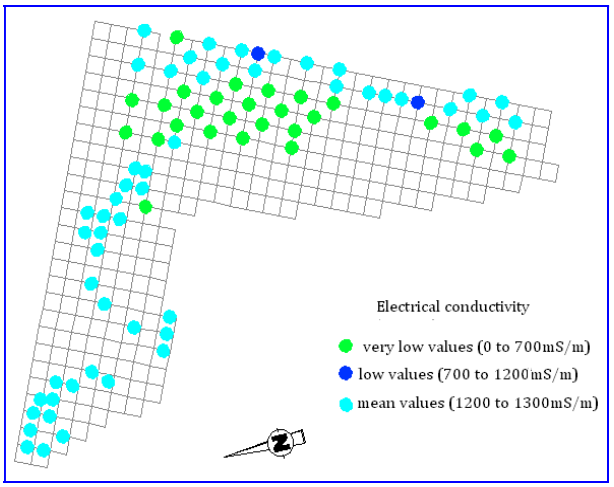

Fig. 8 Distribution of the electrical conductivity on the surface of the infiltration basin.

mS/m. That corresponds to high values of electrical conductivity. The central zone of the large wing of the basin is characterized by low values of electrical conductivity.

4.4 Basin Surface Mapping by Relaxation Time Measurement

In Fig. 9, the yellow color represents a relaxation time lower than 1.4 ns, the red color corresponds to the values ranging between 1.4 ns and 1.6 ns, the green color is for values laying between 1.6 ns and 1.8 ns and the dark blue color represents values higher than 1.8 ns.

The sandy zone located at the north-west of the basin exhibits higher relaxation times analogous to the water content, permittivity and electrical conductivity. Some of the arrears within this zone, which have not been polluted by rather recent fine sand deposits have a relatively mean relaxation time. Measurements indicate values of weak to medium relaxation times in the central part of the northern edge of the basin. In the large wing of the basin, located at the east and extending from the north to the south, covered by alluvia and punctuated by sands, the values of the given relaxation times are generally close to medium values, save for some exceptional points which are associated with weak relaxation times.

5. Distribution of Permeability Coefficient on Pond Surface

The correlations established in the laboratory, between the dielectric parameters and the coefficient of permeability of compacted soil, allow for the determination of the corresponding distribution on the surface of the infiltration basin. This distribution of the coefficient of permeability allows for the localization of the zones of low permeability which delay the infiltration of the storm water which flows in the basin. These zones undergo the deposit of fine grains from which results surface clogging.

According to the results from the laboratory tests, the values of the dielectric parameters facilitate for the prediction of permeability coefficient varying from 2 × 10^{-5} to 10^{-4} m/s. The yellow color corresponds to a coefficient of permeability lower than 2 × 10^{-5} m/s, the red color for the coefficients ranging between 2 × 10^{-5} and 4 × 10^{-5} m/s, the green color for the coefficients ranging between 4 × 10^{-5} and 6.1 × 10^{-5} m/s and the dark blue color corresponds to coefficients higher than 10^{-4} m/s.

The distribution of the colors on the grid of the surface of the basin proves that the most permeable zones are more significant in the large wing of the basin while in the small wing, the points represented by yellow, red and green colors are more dominant (Fig. 10).

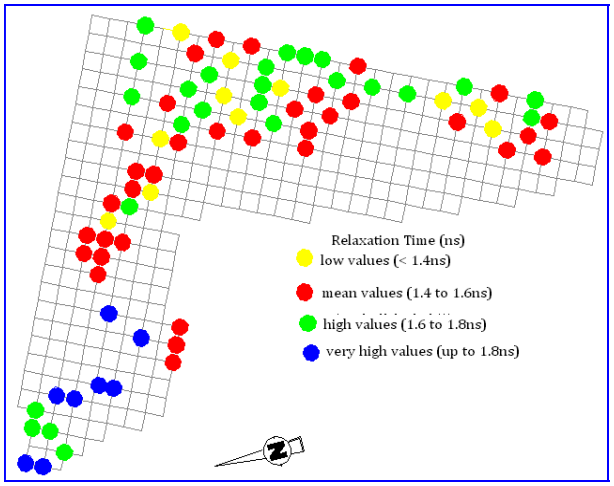

Fig. 9 Distribution of the relaxation time on the surface of the infiltration basin.

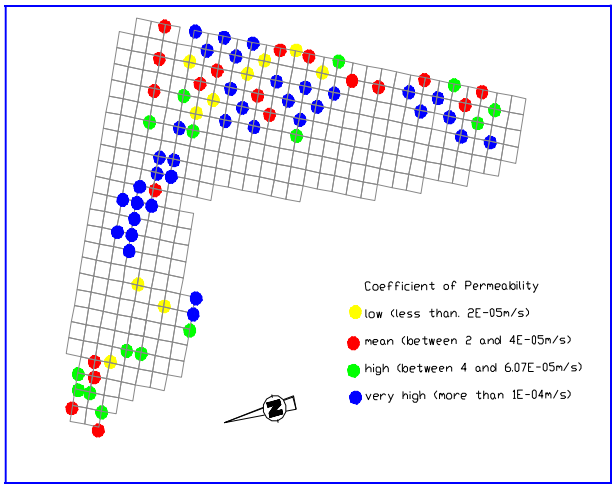

Fig. 10 Distribution of the coefficient of permeability on the surface of the infiltration basin.

It is observed that the clogging can appear in the small surface of the large wing of the basin. However, the fact that these zones are surrounded by more permeable zones indicates that stagnation of water and delays in clogging can be partially mitigated. Implicitly, the small wing of the basin undergoes clogging after each rainy season.

6. Conclusions

The various tests performed in this study showed that it is possible to associate the measurements of the dielectric parameters with the permeability of a compacted soil as has been reported by some researchers. In addition to electrical conductivity, the permittivity and relaxation time parameters can be adopted for this estimate.

This study shows that it is possible to describe the direction of variation of the coefficient of permeability when the dielectric parameters vary. One can thus know the evolution of the coefficient of permeability by following the evolution of the dielectric parameters. The determination of the distribution of the coefficients of permeability on the surface of the infiltration basin allows for the prediction of the zones of stagnation of water after infiltration, depicting zones that characterize clogging. Furthermore, TDR measurements can be used for the detection of these zones. Consequently, the permeability of these zones can be improved by excavation before the rainy season. These measurements can also be used for the management of the infiltration basins for sustainable flood mitigation measures.

References

[1] G.C. Topp, J.L. Davis, A.P. Annan, Electromagnetic determination of soil water content: Measurement in coaxial transmission lines, Water Resour. Res. 16 (1980) 574-582.

[2] O. Mazac, I. Landa, On determination of hydraulic conductivity and transmissivity of granula acquifers by vertical electrical sounding, Journal of Geological Science 16 (1977) 123-129.

[3] M.J.C. van Gemert, High frequency time domain methods in dielectric reflectrometry, Philips Research Reports 28 (1973) 530-572.

[4] T.S. Clarkson, L. Glasser, R.W. Tuxwordth, G. Williams, An appreciation of experimental factors in time-domain spectroscopy, Adv. Mol. Relaxation Interact. Processes 10 (1977) 173-202.

[5] G.C. Topp, J.L. Davis, Time-domain reflectrometry (TDR) and its application to irrigation scheduling, in: D. Hillel (Ed.), Advances in Irrigation, Vol. 3, Academic Press Orlando, USA, 1985, pp. 107-127.

[6] A. Nadler, S. Dasberg, I. Lapid, Time domain reflectometry measurements of water content and electrical conductivity of layered soil columns, Soil Sci. Soc. Am. J. 55 (1991) 938-943.

[7] S. Dasberg, F.N. Dalton, Time domain reflectrometry field measurements of soil water content and electrical conductivity, Soil Sci. Soc. Am. J. 49 (1985) 293-297.

[8] T.J. Heimovaara, E.J.G. de Winter, W.K.P. van Loon, D.C. Esveld, Frequency-dependent dielectric permittivity from 0 to 1 GHz: Time domain reflectrometry measurements compared with frequency domain network analyzer measurements, Water Resourc. Res. 32 (1996) 3603-3610.

[9] J.D. Roades, V. Schilfgaarde, An electrical conductivity probe for determining soil salinity, Soil Sci. Am. J. 40 (1976) 647-651.